THE JOURNAL OF COMPARATIVE NEUROLOGY 462:144–152 (2003)

Marked Loss of Myelinated Nerve Fibers in the Human Brain with Age

LISBETH MARNER,[1]* JENS R. NYENGAARD,[2] YONG TANG,[2] AND BENTE PAKKENBERG[1]

[1]Research Laboratory for Stereology and Neuroscience, Bispebjerg Hospital, 2400 Copenhagen N, Denmark

[2]Stereological Research Laboratory and Electron Microscopy Laboratory, University of Aarhus, 8000 Aarhus, Denmark

ABSTRACT

The white matter is the structure of the brain that declines most with age—almost 30%, but little is known about the age-effect on the fibers that constitute the white matter. In the present study, the total length of myelinated fibers was measured with a newly developed stereologic method. Specimens came from 36 normal Danes (18 males and 18 females) with an age ranging between 18 and 93 years. Samples were taken systematically and randomly from the white matter, and the biopsy specimens were randomly rotated before sectioning to avoid bias due to the anisotropic nature of nerve fibers. The fibers were counted at light microscopic level at approximately 10,000× magnification, and the diameter of each counted fiber was measured to get the diameter distribution. Males were found to have a total myelinated fiber length of 176,000 km at the age of 20 and 97,200 km at the age of 80, whereas the total length in females was 149,000 km at the age of 20 and 82,000 km at the age of 80. This finding corresponds to a 10% decrease per decade or a total decrease of 45% from the age of 20 to 80 years, and a sex difference of 16%. The fiber diameter distribution showed that primarily the thinner fibers were lost with a relative preservation of the thicker ones. The marked loss of myelinated nerve fibers with age could explain some of the cognitive decline seen in the elderly. J. Comp. Neurol. 462:144–152, 2003.

Indexing terms: diameter; axon; stereology; white matter; aging

The interest in white matter in the aging process has increased dramatically after magnetic resonance imaging (MRI) has revealed significant age-related cerebral white matter changes. The percent of a healthy age-population showing one or more hyperintensity lesions on T2-weighted images increases almost linearly from below 20% for individuals 21–30 years of age to 100% for individuals 71–80 years of age (n = 142; Christiansen et al., 1994). These changes are even more common in individuals with Alzheimer's disease or vascular dementia. It is not known whether the pathogenesis is the same in demented and nondemented individuals (Bronge et al., 2002). The most accepted opinion is that white matter changes have an ischemic origin, mainly linked to cerebral small vessel changes (Pantoni, 2002), and this finding corresponds to the correlation between white matter changes and hypertension (Skoog, 1998). The hyperintensity lesion is microscopically characterized by a rarefied appearance of the white matter; loss of myelin, axons, and oligodendrocytes; as well as stenosis of arterioles and smaller vessels similar to that found at the border of true infarcts (Brun and Englund, 1986; Bronge et al., 2002; Pantoni, 2002). The lesion is, however, best characterized in Alzheimer's patients, but the microscopic findings are assumed to be the same in nondemented individuals.

The hyperintensities are rather nonspecific changes, as almost any change in tissue composition will increase the amount of water and, thereby, produce a hyperintense signal (Barkhof and Scheltens, 2002), and the sensitivity

This study was approved by the Danish Ethical Committee, jr. (KF) 01-079/95.

Grant sponsor: Danish Research Council; Grant sponsor: Brd. Hartmann Foundation; Grant sponsor: Lundbeck Foundation.

*Correspondence to: Lisbeth Marner, Research Laboratory for Stereology and Neuroscience, Bispebjerg Hospital, Opg. 11B, 2. Sal, Bispebjerg Bakke 23, 2400 Copenhagen N, Denmark. E-mail: lisbeth@marner.dk

Received 19 July 2000; Revised 11 September 2002; Accepted 11 March 2003

DOI 10.1002/cne.10714

Published online the week of June 2, 2003 in Wiley InterScience (www.interscience.wiley.com).

of MRI is also lower than that of histopathologic examination (Bronge et al., 2002). A more specific approach is diffusion weighted imaging, a newer MRI method that measures the diffusion of water molecules. The restriction of diffusion by white matter tracts can give a measure (the apparent diffusion coefficient, ADC) for the amount of myelinated fibers. Age-studies are still limited in number but tend to show a small increase (<10%) in ADC, suggesting a small decrease in the amount of myelinated fiber tracts in the white matter with age (Engelter et al., 2000; Abe et al., 2002; Helenius et al., 2002). The exact interpretation of the results, however, is not settled. Quantitative autopsy studies of the white matter are scarce and often restricted to smaller regions like the corpus callosum (Meier-Ruge et al., 1992, Aboitiz et al., 1996; Highley et al., 1999).

The general age-related decline in white matter volume points toward a role for white matter in aging. A neuropathologic quantitative study of human aging by using stereologic methods has shown a minor age-related decline in total neocortical neuron number (10%) and neocortex volume (12%) compared with a much larger decline in white matter volume (28%; Pakkenberg and Gundersen, 1997). In vivo studies using MRI also reveal significant age-related losses of white matter volume compared with a much smaller decline in gray matter volume (Albert, 1993; Christiansen et al., 1994; Guttmann et al., 1998; Jernigan et al., 2001).

The combination of a marked loss of white matter with an increasing number of white matter lesions suggests a large nerve fiber loss in the aging process. This study addresses a quantitation of nerve fibers with age by using stereologic methods based on unbiased principles. We chose to study only the myelinated nerve fibers, as most nerve fibers in the central nervous system are myelinated in contrast to the peripheral nervous system (Hildebrand et al., 1993). A newly developed stereologic method (Tang and Nyengaard, 1997) was used to estimate the total volume, total length, and the diameters of myelinated nerve fibers in autopsied brains. A preliminary study of five young and five old females (Tang et al., 1997) showed a decrease of the total length of myelinated fibers with age.

MATERIALS AND METHODS

Materials

The brains were part of a large repository collected from 1987 to 1991 from autopsied individuals following the Danish laws on autopsied human tissue. The brains have been used in a previous study of the neocortical neuron number (Pakkenberg and Gundersen, 1997). The material consisted of brains from 36 normal Danes, 18 males from 19 to 87 years of age (average, 52 years) and 18 females from 18 to 93 years of age (average, 62 years). The brains were selected to cover the age range for both sexes, but the age distributions were not the same, as the brains were sampled consecutively and fewer females than males die young and fewer males than females survive to a high old age. Apart from one case, which was autopsied 96 hours postmortem, all the brains were fixed within 12–72 hours after death and have been fixated for at least 5 months in 4% formaldehyde buffered with phosphate.

In Denmark, people do not move much and the local practitioners and hospital departments know their patients well. The hospital files of the donors, the autopsy report, as well as some files from the local practitioners were carefully studied to exclude individuals with diseases that might affect the central nervous system, such as cerebrovascular diseases, metastatic cancer, diabetes, hypertension, or abuse of alcohol or drugs. The causes of death are listed in Table 1 together with sex, age, brain weight, and possible concurrent illnesses. Despite some chronic medical conditions, all our subjects were functioning normally in their community until shortly before death. Although no cognitive assessment was performed, the hospital staff or their local practitioner regarded them cognitively normal and a thorough neuropathologic examination was performed.

Methods

The brains were coded so that age and gender were unknown to the investigator. The hemispheres were embedded in 6% agar. Right or left hemisphere was chosen systematically at random (19 right and 17 left hemispheres) and cut into 5- to 7-mm-thick slabs starting at the frontal pole with a mean number of slabs per brain of 26 ($CV = SD/Mean = 0.11$). The total volume of white matter, $V(wm)$, from one hemisphere was estimated using the Cavalieri principle: A counting grid with an area per point of 2.25 or 4.5 cm^2 was placed at random on each slab. The points hitting the white matter were counted. The average slab thickness, t, was multiplied by the area per point, $a(p)$, times the total number of points, ΣP, from all slabs, to give the volume of white matter per hemisphere:

$$V(wm) = t \times a(p) \times \Sigma P$$

The total white matter volume per brain was estimated by multiplying by 2. To sample approximately eight slabs per brain, the sampling fraction of slabs was 1:3 or 1:4, depending on the total number of slabs in each brain. A mean of 8.7 slabs per brain ($CV = 0.22$) were sampled systematically by choosing one of the first three (or four) slabs randomly and then every third (or fourth) thereafter. A plastic sheet with equidistantly spaced holes (6.8 cm^2 per hole) was then placed randomly on the caudal surface of the sampled slabs, and 1-mm needle biopsy samples were obtained where the holes in the sheet hit the white matter (Fig. 1). This method resulted in a large variation in the number of biopsy samples per brain, but at least eight biopsies were needed to get reasonably reliable results. If less than eight samples were available from the entire brain, the process was repeated. If more than 14 samples were available, the number of biopsies was systematically reduced in number. A mean of 10.4 biopsy samples were obtained per brain ($CV = 0.19$).

This biopsy technique ensures a uniformly random distribution of the white matter samples and, thereby, provides an equal sampling probability for all parts of the white matter. Thus, the final total number of samples represented all parts of the white matter equally.

A 1-mm length was examined from the original upper end of the cylindrical biopsy sample, rinsed in ion-exchanged water and 0.1 M cacodylate buffer at pH 7.4, and fixed in buffered osmium tetroxide (1%) for 2 hours. Because dehydration with alcohol resulted in up to 50% shrinkage, it was replaced by chemical dehydration with di-methoxy-propane, which markedly reduced the shrink-

TABLE 1. Clinical Details of the Subjects

Sex	Age (yrs)	Brain weight (g)	Cause of death	Concurrent illnesses
Females	18	1,320	Hemorrhage, knife stab	
	30	1,500	Pneumonia	Cancer colli uteri without metastases
	32	1,303	Pulmonary emboli	Breast cancer diagnosed 7 days before death
	39	1,385	Rupture of inferior vena cava (traffic accident)	
	43	1,210	Cardiac insufficiency caused by artificial valve failure	
	47	1,185	Heart failure during by-pass operation	Coronary sclerosis
	53	1,310	AMI	Uncompensated heart failure
	57	1,450	Cardiac insufficiency	Atherosclerosis, hysterosalpingo-oophorectomy
	62	1,450	AMI	Atherosclerosis, bronchitis, emphysema
	64	1,240	AMI	
	72	1,160	AMI	
	72	1,400	Emboli	
	80	970	Cardiac insufficiency	Insufficient mitral valve
	85	1,180	AMI	
	89	1,190	AMI	Diverticulitis, hearing- and walking-impaired
	90	1,040	Pneumonia	Bronchitis
	90	1,310	Diverticulitis with complications	Glaucoma, blindness
	93	1,120	Pulmonary emboli	AMI, pacemaker
Mean	**62**	**1,262**		
	(18–93)	(970–1500)		
Males	19	1,500	Rupture of heart (traffic accident)	
	19	1,460	CO-poisoning in fire	
	22	1,750	Suffocation (abuses spir. Acuta)	
	28	1,400	Hemorrhage, knife stab	
	37	1,616	AMI	
	39	1,550	AMI	
	40	1,620	AMI	Hypertension
	43	1,560	AMI	Calf vein thrombosis
	48	1,290	AMI	By-pass operation
	54	1,670	AMI	AMI × 3
	55	1,160	AMI	Angina pectoris
	60	1,500	AMI	AMI
	67	1,330	Pulmonary emboli	AMI, COLD
	70	1,300	Insufficient respiration	Bronchitis recidivans
	74	1,390	AMI	AMI, COLD
	81	1,390	Ulcus ventriculi	Ulcus ventriculi
	84	1,280	Bronchopneumonia and AMI	
	87	1,330	AMI	
Mean	**52**	**1,450**		
	(19–87)	(1,160–1,750)		

AMI, acute myocardial infarction; COLD, chronic obstructive lung disease.

Fig. 1. Sampling of a biopsy specimen. A grid with equidistantly spaced holes on top of a slab of brain. The tissue is biopsied where the holes hit white matter.

age. The tissue was embedded in 3-mm Epon spheres, and the spheres rotated randomly before re-embedding (Nyengaard and Gundersen, 1992). This procedure ensures isotropic, uniform, and random sections, so that each biopsy sample has a uniformly random orientation before cutting. This approach is essential for the length measurements to avoid methodologic bias due to the anisotropic orientation of the myelinated fibers.

By using an ultramicrotome, 100-nm-thick sections were cut from each biopsy specimen and stained with 1% toluidine blue. The sections have to be very thin to avoid projection bias. This bias increases the closer the size of the examined structure is to the section thickness. The thinnest myelinated fibers are only two to three times thicker than the sections, which is why a small overestimation of the volume density must be expected (Gundersen, 1979). Quantification was performed by using an Olympus light microscope with 100× oil immersion objective and a video camera. The camera signal is overlaid with a grid from a computer (using GRID 1.2 software) through a genlock card and displayed on a television screen at a total magnification of approximately ×10,000. The myelin sheath is rather unaffected by postmortem autolysis and was used as the counting item. We identified the sheaths as dark blue rings with the holes being a little darker than the surrounding tissue and with the thickness increasing with the diameter of the fiber. The thinnest fibers are the most difficult to recognize, as their diameter is at the resolution limit of the light microscope. The myelinated axons in the central nervous system have diameters down to 0.2 μm, whereas the unmyelinated axons have diameters up to 0.8 μm. This finding is in contrast to the peripheral nervous system, in which the

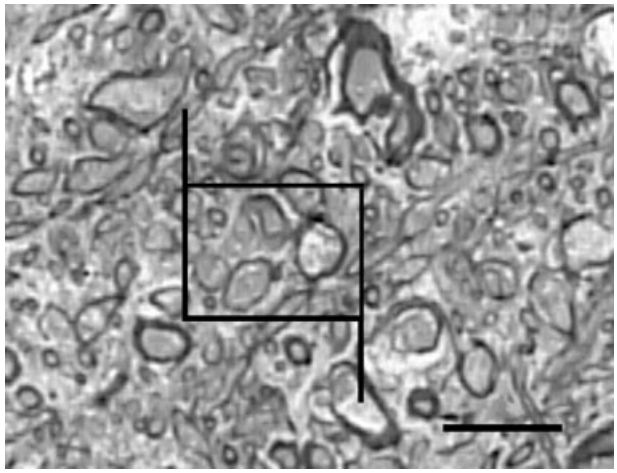

Fig. 2. Fibers counted at approximately 10,000× magnification by using light microscopy. A computer provided an unbiased counting frame of approximately 25 μm^2. The blurred profiles are due to the high magnification. See text for details. Scale bar = 5 μm.

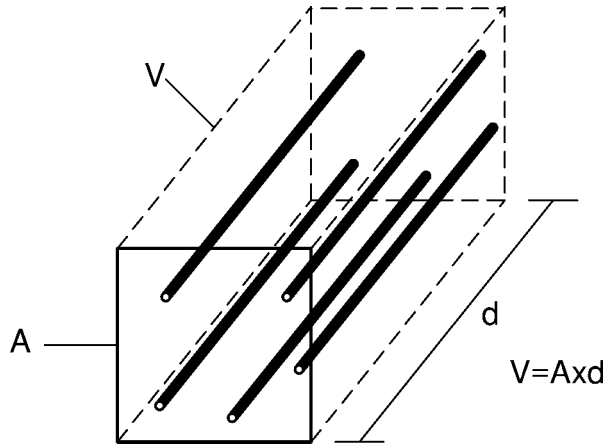

Fig. 3. Illustration of formula showing box with parallel fibers. A, area of box; V, volume of box; d, depth of box. See text for details.

lower limit for myelination is approximately 1-μm diameter.

To evaluate the criteria for identification of myelin sheaths, we compared consecutive sections by using a light microscope and electron microscopic pictures taken at the same magnification, and identified the corresponding fibers. Differences of less than 5% were found when comparing estimates of the total length from the light microscope and the electron microscopic pictures (for details, see Tang and Nyengaard, 1997). The possible changes caused by the postmortem autolysis and formaldehyde fixation could not be monitored. Measurements over time, however, showed no postmortem changes in nerve fiber parameters in a dog and a pig brain (Tang and Nyengaard, 1997).

Of the 10.4 biopsy samples per hemisphere, the usable number of samples per brain was 9.7. The remaining 7% turned out to be gray matter or was excluded due to massive artifacts or poor staining.

The total length of nerve fibers may seem an unfamiliar measure. A simple cut through the white matter, counting fibers per area, will only give information about the number of fibers passing more or less perpendicularly through this area. Other fiber directions and the volume changes of white matter (due to preparation or age-changes) are important parameters, which are included in the total length estimation; as the specimens are systematically randomly biopsied, the tissue is randomly rotated and the volume of white matter is measured.

The counting was performed by using the so-called unbiased counting frames (Gundersen, 1977; Fig. 2). These are designed to avoid any bias due to size and shape of the objects. Objects inside the counting frame or touching the top and right lines are included (thin inclusion lines) and objects touching the bottom and left lines are excluded (thick exclusion lines). This design takes the higher probability of large objects to occur in a counting frame into account. The thick exclusion lines are extended so that for instance the amount of snakelike objects will not be overestimated. To fully understand the concept of the unbiased counting frame, one must imagine the entire section divided into counting frames lying side by side. Each specimen must only be sampled in one of the counting frames and must be excluded if it appears in any other counting frame. The number of fiber profiles per area was counted in such unbiased counting frames (60 μm^2) placed in each of the four corners of the sections avoiding major artifacts (cracks, discoloring, etc.). The positions were chosen at low magnification so that the examiner could not prefer one area to another. In sections with a random orientation, the length density, L_V, is the total length of fibers per volume of white matter. It is estimated from

$$L_v = \frac{2 \times \text{Total number of counted nerve fiber profiles}}{\text{Total sampling area} \times (1 + \text{average area shrinkage})}$$

and the total length is estimated from

$$\text{Total length} = L_v \times V(WM)$$

V(WM) being the volume of the white matter (Gundersen, 1979).

In the following, we will aim at making the formula more intuitively obvious. Imagine that the fibers passing perpendicularly through an area A were all straight and cut in parallel. A box of white matter with one end being the area A and with the depth d has the volume $V = A \times d$ (Fig. 3). The total length of fibers L in this box would be the number of fibers multiplied by d, and the length density, i.e., the total length per volume, would be

$$\text{“Length density”} = \frac{L}{V} = \frac{\text{number of fibers} \times d}{A \times d} = \frac{\text{number of fibers}}{A}$$

Because nerve fibers in white matter are not parallel, this formula underestimates the length density. The constant “2” in the correct formula comes from the 50%

chance for a fiber in three-dimensional space to be intersected by a uniformly randomly orientated plane.

By using a grid with 30 equidistantly spaced points and an area per point of 34 μm^2, the volume density V_V of nerve fibers, i.e., the volume of fibers per volume of white matter, was estimated as the fraction of points on the section hitting nerve fibers, including their myelin sheaths (Gundersen, 1979)

$$V_v = \frac{\text{Total number of points hitting nerve fibers}}{\text{Total number of points hitting white matter}}$$

An average of 310 fibers (range, 150–556 fibers) were counted per brain with an average coefficient of error ($CE = SEM/Mean$) of 0.11 on the estimate of the total length. The variance between the sections determines the minimum number of sections per brain, and the variance between the counting frames in each section determines the optimal number of counting frames. A coefficient of error of approximately 10% was regarded as optimal. If larger, the data are too uncertain; if lower, the extra work would have been spent more efficiently by studying more brains, as the biological variance is very high. It may be surprising that an average of less than 10 small biopsy samples per brain and a count of 300 myelin sheath profiles can give a sufficient estimation of the total length in the entire white matter. The answer lies in the strictly uniform sample technique and the simple fact that the sampling precision is independent of the sampling fraction (which is very low in this study) but is determined by the sample size.

To ensure that the identification of nerve fibers was reliable and reproducible, three brains were recounted. The densities of the brains were 261, 237 and 288 m/mm^3 at the first counting and 268, 277, and 285 m/mm^3 at the second. We judge this difference as negligible.

The diameter of each fiber counted was measured at right angles to the maximum width of the fiber profile (Gundersen, 1979), and measurements were obtained from the outer limit of the myelin sheath with a precision of 0.1 μm.

To measure the shrinkage, three extra biopsy samples from each brain were sampled. They were sampled next to three of the earlier sampled biopsy specimens chosen systematically randomly. A small cube of tissue was cut out, and a needle biopsy was performed from the cube in sagittal, frontal, or horizontal orientation so that each brain is represented by all three orientations. From each of the cylindrical biopsy samples, the top 1-mm cylinder of white matter was carefully separated from the rest of the cylinder and the cross-sectional area was measured in a light microscope. The cylinders were fixated and dehydrated together with the rest of the specimens from that particular brain. Sectioning was carefully performed perpendicularly to the length of the cylinder. After staining, the area was measured again and the area of shrinkage was estimated. The area of shrinkage for each brain and the average area of shrinkage for each of the three orientations from all the brains were calculated. The average area of shrinkage was found to be 5.9% ($P = 0.001$) and independent of orientation. As the shrinkage did not show any correlation with age or sex, the average area of shrinkage was used to correct the length density estimates.

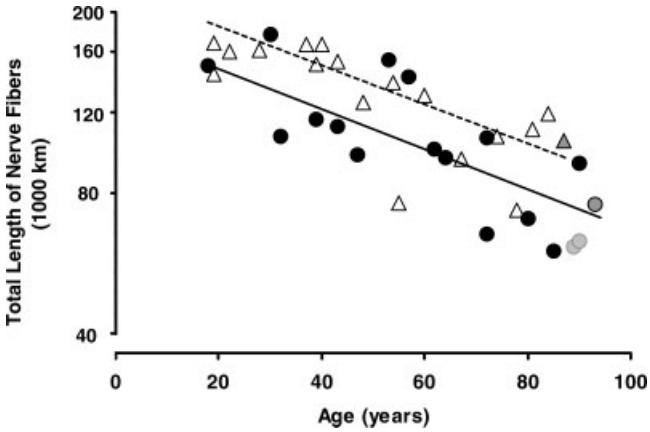

Fig. 4. Total length of myelinated fibers on a logarithmic scale as a function of age for males (triangles) and females (circles). The regression lines with a common slope of 1.01% per year are indicated for males (dashed line) and females (solid line). The subjects showing neuropathologic changes in the hippocampal region are depicted by the gray filled triangle and encircled gray circle, whereas the subjects with changes in the cortex as well are depicted by non-encircled gray circles.

Neuropathology. After the specimens were gathered for counting, tissue blocks were biopsied from the same hemispheres from the frontal, parietal, medial, temporal, and occipital lobes; insula; gyrus cinguli; hippocampus; and one or two tiers of mesencephalon. Cerebellum was not examined. The tissue was processed routinely and embedded in paraffin wax. Four-micron-thick sections were cut from all blocks for hematoxylin and eosin stains, and for immunohistochemistry from selected areas. Eight-micron-thick sections were cut from all blocks for Kluver-Barrera staining. Immunohistochemistry included beta-amyloid (DAKO, Glostrup, Denmark, M0872 1:200), tau (DAKO, Glostrup, Denmark, A0024 1:50,000), ubiquitin (DAKO, Glostrup, Denmark, Z0458 1:5,000), and alpha-synuclein (Zymed, San Francisco, CA, 18-0215 1:2,000). Some of the aged brains showed a degree of cortical and cerebral atrophy, with the basal ganglia being normally proportioned without discoloring. The brainstems were normal, including pigmentation of substantia nigra. There were no tumors or hemorrhages. No brains showed cortical spongiosis, abnormal neuronal or glial inclusions, vasculitis, or encephalitis. Only four of the subjects (87, 89, 90, and 93 years of age) showed scattered senile plaques and amyloid deposits: two in the hippocampal region only and two in cortex as well. Because no concomitant clinical signs of dementia were reported, and these pathologic changes also are seen in normal old age (Esiri et al., 1997), the subjects were not excluded from the study (see also results and Fig. 4). Preclinical states of Alzheimer's disease can of course not be excluded.

Statistics

Because most biological variables vary in an exponential manner, all continuous variables (except age) were analyzed after logarithmic transformation. A significance level of $P = 0.05$ was adopted throughout.

Age-adjusting was performed when comparing two parameters that both vary with age. The age-adjusted total length was calculated for each person, i, as

TABLE 2. Results

Parameter	% Sex difference	Sex	% Loss per decade (% loss from 20 to 80 years)	20 years of age	80 years of age
Total length of fibers (km)	16*	Males	10*** (45)	176,000	97,200
		Females	10**** (45)	149,000	82,000
Volume of white matter (ml)	13*	Males	4.3 (23)	550	423
		Females	4.3* (23)	484	372
Fiber length density, Lv (km/ml)	3.5	Males	5.8** (29)	321	229
		Females	5.8*** (29)	310	221
Total volume of fibers (ml)	17**	Males	5.9** (29)	217	153
		Females	5.9** (29)	182	128
The volume density, Vv (fraction)	4.5	Males	1.58 (9)	0.40	0.36
		Females	1.58 (9)	0.38	0.34

[1]Probability data are presented as follows: *$P < 0.05$; **$P < 0.01$; ***$P < 0.001$; ****$P < 0.0001$.

$$\text{total length}_i \times e^{b(\text{mean age} - \text{age}_i)}$$

b being the slope of the regression line of the chosen parameter vs. age.

To analyze changes in fiber size with age and sex, the distribution of fiber length vs. diameter was first determined. This absolute diameter distribution allows us to see actual changes. It was calculated as follows: Based on the smallest and the largest diameter values, 13 classes of equal width were calculated after logarithmic transformation. For each person, the total fiber length in each diameter class was calculated by multiplying the fraction of fibers of each diameter class with the total length of fibers for that individual. The mean length of fibers and standard error of the mean were determined for each class for "young" (<45 years) and "old" (≥70 years) males and females.

Comparison of the fiber loss for the varying fiber diameters, however, is difficult with the logarithmic distribution, as the length of fibers in the very small and very large diameter classes are too small for tests of significance. To get samples of equal size, the diameters were divided into quintiles. The following describes how we calculated these quintiles. The overall fiber diameter distribution was first computed for males and females separately to test for sex differences. If the age distribution of the 18 individuals of each sex had been uniform, individual observations should weigh 1/18 in this computation. This was not the case. Among the females, five were young (age <45 years), five were "middle-aged" (45 years ≤ age <70 years), and eight were old (age ≥70 years), whereas the male distribution was eight, five, and five, respectively, by using the same age-ranges (Table 1). Instead of 1/18, each individual was given a weighting of 1/(3n), where n is the number of individuals in the age group. The number of fibers (N) counted per individual varies, so each fiber ended up with a weighting of $1/(3n \times N)$. The two distributions were compared with regard to their weighted geometric mean using an unpaired two-sided Student's t test. As the sexes did not show any significant differences in their distribution, their measurements were pooled, and the overall diameter distribution and its quintiles were calculated using the same weightings. The quintiles of the complete material were used to calculate the total fiber length of the five quintiles for each individual. The mean total length of fibers and the standard error of the mean were computed for young and old males and females and plotted as a function of quintile number. The fiber loss with age was calculated as the difference between young and old in mean length, and this calculation was also plotted as a function of quintile number for males and females.

RESULTS

On average, males at age 20 have a total length of 176,000 km of myelinated fibers and lose 79,200 km with age to 97,200 km at the age of 80. Females at age 20 have a total myelinated fiber length of 149,000 km and lose 67,000 km with age to 82,000 km at the age of 80. A regression of the total length of nerve fibers on age revealed negative regression coefficients significantly different from zero in both males ($P = 0.0007$) and females ($P = 0.00008$).

Males were found to have 16% longer total length of myelinated fibers ($P = 0.02$), but the sexes showed no difference ($P = 0.32$) in the relative loss per decade, which was 10% per decade or 45% from the age of 20 to 80 (Fig. 4). The four cases with neuropathologic changes had no impact on the results. The biological variation is large with coefficients of variation ($CV = SD/Mean$) for the total length of 0.34 for females and 0.24 for males. Even after removing the variance from age differences, the CV is still 0.22 among females and 0.17 among males.

From the regressions of white matter volume, length density (length per volume of white matter), the total volume of fibers, and volume density (volume of myelinated fibers per volume of white matter) on age, the calculated loss from the age of 20 to 80 and the sex differences are shown in Table 2. The volume density was not significantly changed by age or sex ($P = 0.32$ and $P = 0.37$, respectively).

A significant correlation between age-adjusted brain weight and age-adjusted total length of myelinated fibers was found for both males ($r = 0.58$; $P = 0.01$) and females ($r = 0.62$; $P = 0.006$).

The average geometric mean diameter increases by 13% ($P = 0.005$) with age from 0.79 μm at the age of 20 to 0.89 μm at the age of 80 for both sexes. The absolute size distribution for young and old subjects of each sex is shown in Figure 5 and suggests a loss of the fibers smaller than 1.5 μm and no gain of the thicker ones; hence, fibers are not just getting thicker.

The age-adjusted distribution showed no difference in geometric mean fiber diameter between males (0.86 μm) and females (0.85 μm; $P = 0.95$), and an overall distribution adjusted for age and sex was computed and its quintiles established.

The difference between young and old, i.e., absolute fiber loss with age, was significantly correlated to quintile number for females ($r = -1.00$; $P = 0.000001$) and males

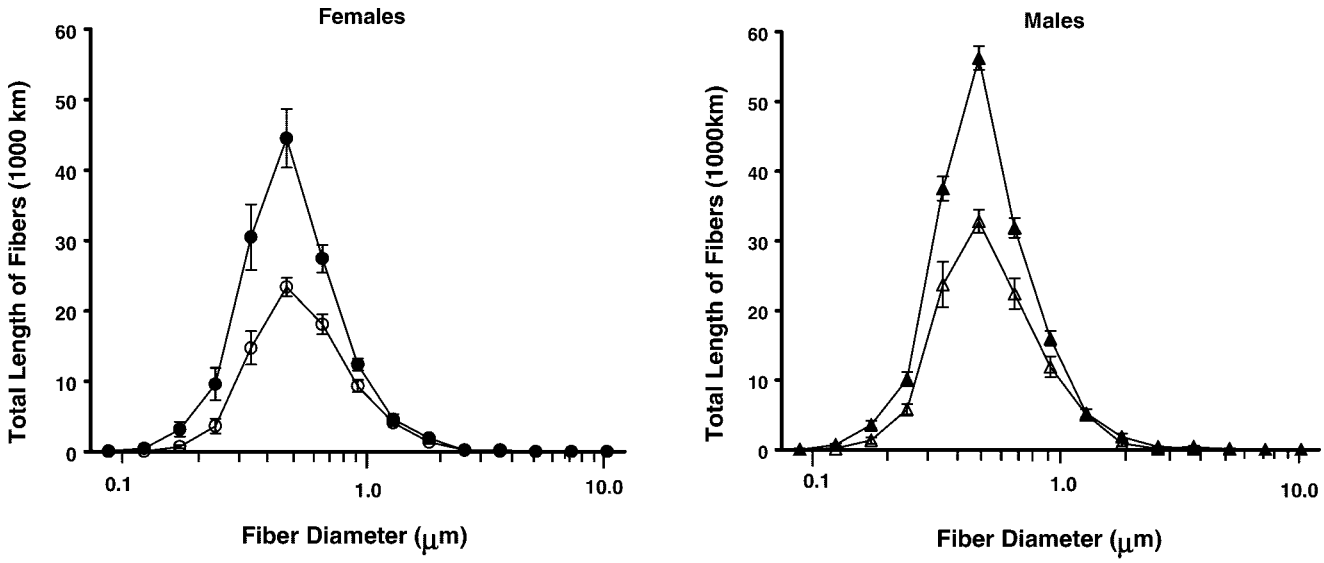

Fig. 5. The absolute diameter distribution of fibers separated for "young" (≤45 years of age; filled circles) and "old" (≥70 years of age; open circles) females and "young" (filled triangles) and "old" (open triangles) males. The total length of myelinated fibers is shown as a function of diameter on a logarithmic scale. Thirteen classes of fibers are shown with the width of each class being 38% of the local mean diameter. The standard errors are indicated.

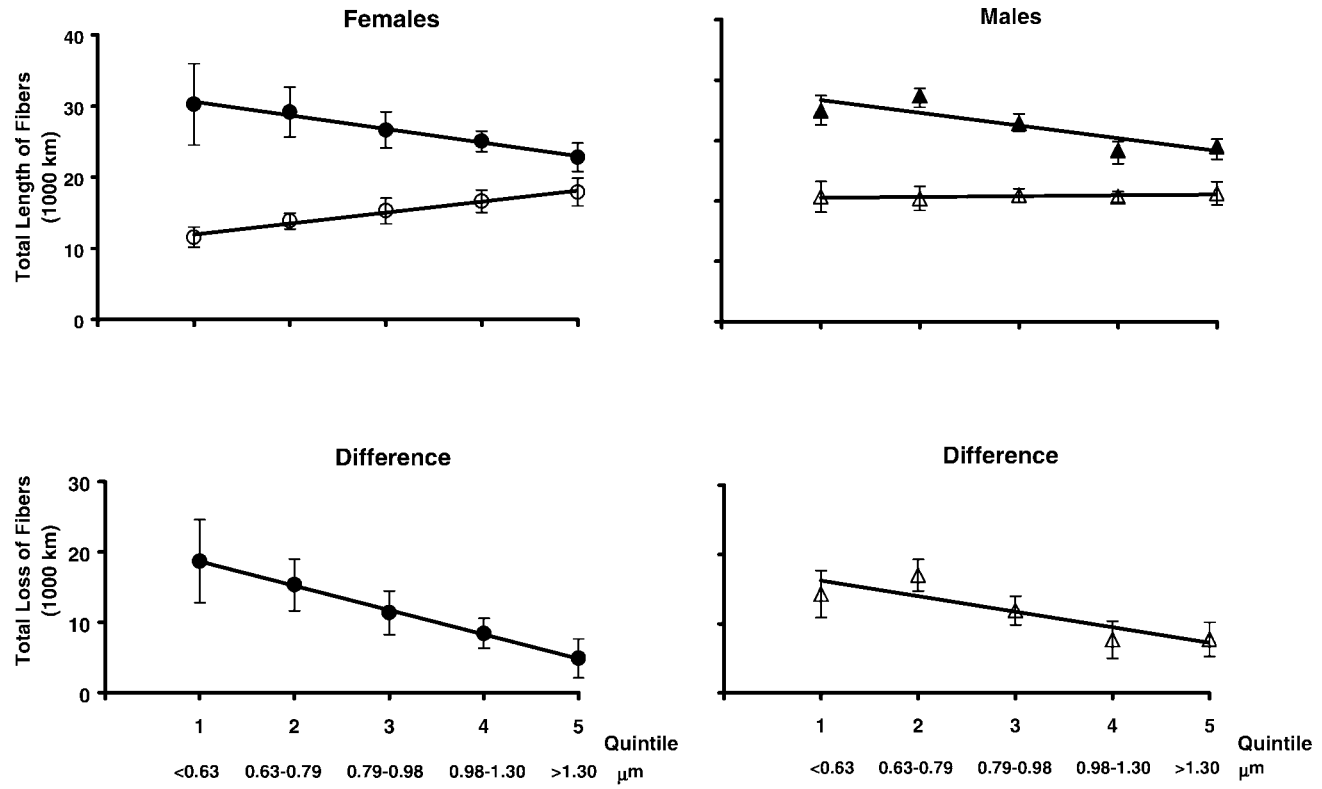

Fig. 6. Top: The total length of fibers is shown as a function of quintile number for "young" (≤45 years of age; filled circles) and "old" (≥70 years of age; open circles) females and "young" (filled triangles) and "old" (open triangles) males. The quintiles are based on the overall age- and sex-adjusted diameter distribution of the nerve fibers. Bottom: The differences between "young" and "old" are shown. The regression lines and standard errors of the means are indicated.

($r = -0.87$; $P = 0.03$; Fig. 6). The total length of myelinated fibers did not show any correlation with the cause of death, fixation delay, storage time, right/left hemisphere, or height/weight of the individual.

DISCUSSION

The present findings indicate that normal Danes from the age of 20 to 80 lose 45% of their total length of myelinated fibers in the brain white matter. The reduction increases the smaller the fibers are and progresses steadily from the age of 20. The sexes showed no difference in diameter distribution, but males have 16% longer total length of fibers than females, which corresponds to a 16% difference in total neocortical neuron number (Pakkenberg and Gundersen, 1997). It should be emphasized that these findings relate to the myelinated fibers. We have no data regarding the unmyelinated fibers, and the loss of white fiber length could theoretically be a result of demyelination with preserved axons.

Limitations of the study include shrinkage artifacts that, to our knowledge, are unavoidable. This problem can only be solved by vigorous measuring and corrections. An area shrinkage of less than 6% is low compared with the biological variance of the total length of myelinated fibers, and the shrinkage showed no correlation to age or sex. As most shrinkage is due to disappearance of water (Blinkow and Glezer, 1968), the fatty myelinated fibers are rather unaffected regarding total length and diameter. So when we have corrected the sampling area for shrinkage (see the formula for length density), the result is most likely reliable.

The advantage of the study includes the use of recent stereologic methods that avoid bias from sampling only from selected regions—questioning the generalization of the findings—and measurements not accounting for the marked anisotropy of the fibers. The material is rather homogenous in its size and composition and the consecutive collection of brains from autopsies ensures that the material represents the normal Danish population with individuals representative of their age-cohort in terms of various health concerns and disease histories. This is not entirely true for the young individuals, as it is not very "normal" to die young, but these individuals would only bias the material toward a less marked age difference. No cognitive assessment of the individuals was made, as it lies beyond the scope of this study to correlate fiber length to mental capacity. This means that we cannot definitely rule out that some cases had preclinical stages of dementia. However, a low mental capacity of the individuals included was not noted by hospital doctors or local practitioners, and the neuropathologic examination only revealed four cases of the very oldest with scattered senile plaques and amyloid deposits.

The loss of total fiber length with age is due to a 23% decrease in white matter volume and a 29% decrease in length density, i.e., fiber length per volume. Hence, measuring the total length of myelinated fibers reveals a much more pronounced age-related loss than the previously described loss of white matter volume indicates. Part of this loss could be due to secular trends. During the past century, the brain has increased in size like the rest of the body. Recordings of body and brain weights of autopsied individuals from London during the past century report changes in brain weights of approximately 5% (Miller and Corsellis, 1977). Most likely, secular trends can explain up to 5% of the changes in total length of nerve fibers with age, whereas the remaining 40% probably is an actual decrease in the number of neuronal connections.

The large reduction in connections is matched by a moderate loss of neocortical neurons (10%; Pakkenberg and Gundersen, 1997), and loss of collaterals may explain part of the high loss of fiber length with age. Alternatively, the white matter could be the pathologic site corresponding to the numerous white matter lesions seen on MRI. Supporting this view is the finding that the oligodendrocytes rather than the neurons are affected by age (Peters, 1996; Peters et al., 2000). In aged monkeys, the oligodendrocytes showed numerous age-changes; contained inclusions and myeloid bodies; were often found in pairs, groups, or rows close to capillaries; and the myelin sheaths were falling apart or ballooning. Furthermore, evidence suggests (Ludwin, 1997) that the oligodendrocytes are very susceptible to ischemia and substances produced by the microglia such as cytokines and nitric oxide. Conclusively, cerebral small vessel changes could result in an inability of the oligodendrocytes to maintain their sheaths.

The fibers show a considerable variability in diameter and, thereby, speed of conduction, but except for some relation to the length of the fiber, the functional significance of this variability is unknown (Nieuwenhuys, 1998). The myelinated fibers probably get a thicker myelin sheath with age. Findings show that myelination starts in the 26th week of fetal life, but the cerebral areas devoted to higher functions undergo myelination much later, and myelination is not complete until the second or third decade of life or possibly even later (Filley, 1998; Sowell et al., 1999). Studies of monkey cortices show that the production of myelin lamellae is continued throughout life together with some degeneration. The mean number of lamellae increases mostly due to an increase in the number of fibers with more than 10 lamellae (Peters et al., 2001). Although the myelination is a life-long process, the extent of this thickening is not known in humans and our findings show no increase in the total length of thicker fibers with age.

The reason for the preferential loss of thinner fibers is unknown, but a rather speculative explanation could be that damage to an oligodendrocyte affects more fibers the smaller they are. In contrast to Schwann cells in the peripheral nervous system, one oligodendrocyte is able to myelinate numerous axons through independent processes. The axons myelinated by the same oligodendrocyte are rather uniform with respect to diameter and number of myelin lamellae, and the oligodendrocytes myelinate more fibers the smaller diameter they have (Bjartmar et al., 1994). Other possibilities include loss of collaterals that are thinner than the main axon or that important neurons keep rebuilding and strengthening their axons while the rest degenerate, leaving only the important thicker fibers. The last hypothesis would also explain why most old people still manage to function sufficiently despite a major loss of nerve fibers.

The volume density, i.e., volume of fibers per volume of white matter, is found to be independent of age, which was unexpected considering a decrease in length density of 29%. The reason is the preferential loss of the smaller fibers. The remaining fibers have a constant packing density, and the volume of the lost thinner fibers matches the 23% loss of white matter volume. Because an earlier study of the same brains found no age-related changes in the neocortical neuron density (Pakkenberg and Gundersen, 1997), the fraction of intercellular substance is generally

not changed by age. This may account for the very small changes encountered in diffusion weighted imaging that do not match the actual decline in fiber length with age. A volume density of around 37% may seem lower than expected, but there is a limit to the packing density of fibers, first, because of their round structure, and second, because of their differences in orientation.

It is not obvious what consequences the white fiber loss has for the elderly. The communicative function of the white matter suggests that diffuse white matter pathology would preferentially disrupt more integrative functions of the brain, and especially the frontal lobe function is dependent on the reciprocal connections to the other three lobes (Filley, 1998). The most consistent finding of mental decline is a relatively stable capacity to manipulate information in immediate or primary memory, but with affection of sustained attention. This finding corresponds to the general slowing of the elderly and the fact that, in many tests, the elderly perform correctly but require more time to complete the test (Filley and Cullum, 1994).

Could these deficits be due to the loss of myelinated fibers with age? Patients with white matter diseases (e.g., multiple sclerosis, leukoencephalopathy, Binswanger's disease) often develop dementia, and their symptoms are of the same nature as those of the aged. Filley (1998) concludes in a review that especially the affection of sustained attention and the preservation of language abilities is characteristic of white matter dementia. Commonly allied with deficits in sustained attention is slowed information processing, and in this respect, white matter dementia appears to mimic the effects of normal aging. Deficits in memory retrieval, visuospatial skills, frontal lobe function, and psychiatric status and preserved procedural memory and extrapyramidal function are also features of white matter dementia (Filley and Cullum, 1994).

Possibly, the substantial loss of white fibers in the aging brain could be one of the main reasons for the cognitive decline seen in the elderly, but to date, it is not known how great an impact it has on the maintenance of our mental capacity or how this potentially harmful age-effect may be prevented.

ACKNOWLEDGMENTS

We thank H.J.G. Gundersen for extensive help and advice with statistics, stereology, and methods. We also thank H.J. Jensen, N. Johansen, and S. Primdahl for their technical assistance, and J. Marner for computer assistance.

LITERATURE CITED

Abe O, Aoki S, Hayashi N, Yamada H, Kunimatsu A, Mori H, Yoshikawa T, Okubo T, Ohtomo K. 2002. Normal aging in the central nervous system: quantitative MR diffusion-tensor analysis. Neurobiol Aging 23:433–441.

Aboitiz F, Rodriguez E, Olivares R, Zaidel E. 1996. Age-related changes in fibre composition of the human corpus callosum: sex differences. Neuroreport 7:1761–1764.

Albert M. 1993. Neuropsychological and neurophysiological changes in healthy adult humans across the age range. Neurobiol Aging 14:623–625.

Barkhof F, Scheltens P. 2002. Imaging of white matter lesions. Cerebrovasc Dis 13(Suppl)2:21–30.

Bjartmar C, Hildebrand C, Loinder K. 1994. Morphological heterogeneity of rat oligodendrocytes: electron microscopic studies on serial sections. Glia 11:235–244.

Blinkow SM, Glezer II. 1968. The human brain in figures and tables: a quantitative handbook. New York: Plenum Press. p 1–34.

Bronge L, Bogdanovic N, Wahlund LO. 2002. Postmortem MRI and histopathology of white matter changes in Alzheimer brains. Dement Geriatr Cogn Disord 13:205–212.

Brun A, Englund E. 1986. A white matter disorder in dementia of the Alzheimer type: a pathoanatomical study. Ann Neurol 19:253–262.

Christiansen P, Larsson HB, Thomsen C, Wieslander SB, Henriksen O. 1994. Age dependent white matter lesions and brain volume changes in healthy volunteers. Acta Radiol 35:117–122.

Engelter ST, Provenzale JM, Petrella JR, DeLong DM, MacFall JR. 2000. The effect of aging on the apparent diffusion coefficient of normal-appearing white matter. AJR Am J Roentgenol 175:425–430.

Esiri MM, Hyman BT, Beyreuther K, Masters CL. 1997. Ageing and dementia. In: Graham DI, Lantos PL, editors. Greenfield's neuropathology. 6th ed. New York: Oxford University Press, Inc. p 156–170.

Filley CM. 1998. The behavioral neurology of cerebral white matter. Neurology 50:1535–1540.

Filley CM, Cullum CM. 1994. Attention and vigilance functions in normal aging. Appl Neuropsychol 1:29–32.

Gundersen HJG. 1977. Notes on the estimation of the numerical density of arbitrary profiles: the edge effect. J Microsc 111:219–223.

Gundersen HJG. 1979. Estimation of tubule or cylinder L_V, S_V and V_V on thick sections. J Microsc 117:333–345.

Guttmann CR, Jolesz FA, Kikinis R, Killiany RJ, Moss MB, Sandor T, Albert MS. 1998. White matter changes with normal aging. Neurology 50:972–978.

Helenius J, Soinne L, Perkio J, Salonen O, Kangasmaki A, Kaste M, Carano RA, Aronen HJ, Tatlisumak T. 2002. Diffusion-weighted MR imaging in normal human brains in various age groups. Am J Neuroradiol 23:194–199.

Highley JR, Esiri MM, McDonald B, Cortina-Borja M, Herron BM, Crow TJ. 1999. The size and fibre composition of the corpus callosum with respect to gender and schizophrenia: a post-mortem study. Brain 122:99–110.

Hildebrand C, Remahl S, Persson H, Bjartmar C. 1993. Myelinated nerve fibers in the CNS. Prog Neurobiol 40:319–384.

Jernigan TL, Archibald SL, Fennema-Notestine C, Gamst AC, Stout JC, Bonner J, Hesselink JR. 2001. Effects of age on tissues and regions of the cerebrum and cerebellum. Neurobiol Aging 22:581–594.

Ludwin SK. 1997. The pathobiology of the oligodendrocyte. J Neuropathol Exp Neurol 56:111–124.

Meier-Ruge W, Ulrich J, Bruhlmann M, Meier E. 1992. Age-related white matter atrophy in the human brain. Ann N Y Acad Sci 673:260–269.

Miller AK, Corsellis JA. 1977. Evidence for a secular increase in human brain weight during the past century. Ann Hum Biol 4:253–257.

Nieuwenhuys R. 1998. Structure and organisation of fibre systems. In: The central nervous system of vertebrates. New York: Springer. p 113–157.

Nyengaard JR, Gundersen HJG. 1992. The isector: a simple and direct method for generating isotropic, uniform random sections from small specimens. J Microsc 165:427–431.

Pakkenberg B, Gundersen HJG. 1997. Neocortical neuron number in humans: effect of sex and age. J Comp Neurol 384:312–320.

Pantoni L. 2002. Pathophysiology of age-related cerebral white matter changes. Cerebrovasc Dis 13(Suppl)2:7–10.

Peters A. 1996. Age-related changes in oligodendrocytes in monkey cerebral cortex. J Comp Neurol 371:153–163.

Peters A, Moss MB, Sethares C. 2000. Effects of aging on myelinated nerve fibers in monkey primary visual cortex. J Comp Neurol 419:364–376.

Peters A, Sethares C, Killiany RJ. 2001. Effects of age on the thickness of myelin sheaths in monkey primary visual cortex. J Comp Neurol 435: 241–248.

Skoog I. 1998. A review on blood pressure and ischaemic white matter lesions. Dement Geriatr Cogn Disord 9(Suppl 1):13–19.

Sowell ER, Thompson PM, Holmes CJ, Jernigan TL, Toga AW. 1999. In vivo evidence for post-adolescent brain maturation in frontal and striatal regions. Nat Neurosci 2:859–861.

Tang Y, Nyengaard JR. 1997. A stereological method for estimating the total length and size of myelin fibers in human brain white matter. J Neurosci Methods 73:193–200.

Tang Y, Nyengaard JR, Pakkenberg B, Gundersen HJG. 1997. Age-induced white matter changes in the human brain: a stereological investigation. Neurobiol Aging 18:609–615.